

**Relaxation, nucleation, and glass transition in supercooled liquid Cu**H. Pang,<sup>1,\*</sup> Z. H. Jin,<sup>2,1</sup> and K. Lu<sup>1</sup><sup>1</sup>*Shenyang National Laboratory for Materials Science, Institute of Metal Research, Chinese Academy of Sciences, Shenyang 110016, People's Republic of China*<sup>2</sup>*Max-Planck-Institut für Metallforschung, D-70569 Stuttgart, Germany*

(Received 4 September 2002; published 31 March 2003)

Using molecular-dynamics simulation with the embedded atom method, the dynamical properties of supercooled liquid Cu were studied by characterizing several time-correlation functions. With increasing undercooling of the liquid Cu below the melting point, self-diffusion slows down along with an increase in the structural relaxation time as compared with the normal liquid state. A massive structural rearrangement leading to incipient nucleation for crystallization occurs at a certain supercooling and time, underlying the existence of a transition in dynamical heterogeneities. Based on the temperature dependence of the characteristic relaxation times, a time-temperature-nucleation diagram has been constructed by which the relaxation, nucleation, and glass transition can be consistently correlated.

DOI: 10.1103/PhysRevB.67.094113

PACS number(s): 61.20.Ja, 64.70.Pf

**I. INTRODUCTION**

Though metallic liquids normally crystallize on cooling below the melting points, they can undergo glass transition or vitrification if the cooling rate is fast enough to suppress the nucleation and growth of the crystalline phase.<sup>1</sup> It is emphasized that the competition between crystallization and vitrification plays the most important role during supercooling, which was summarized by Angell<sup>2</sup> to be the result of the interplay between two characteristic times  $\tau_1$  and  $\tau_2$ .  $\tau_1$  is the time necessary to convert a certain volume fraction of a liquid to the crystalline phase. During cooling between  $T_m$  (the equilibrium melting temperature) and  $T_g$  (the glass transition temperature),  $\tau_1$  first decreases, reaching a minimum  $\tau_1^*$ , and then increases with the extent of supercooling. The nonmonotonic relationship between  $\tau_1$  and  $T$  is straightforward by the classical nucleation and growth theory<sup>1,3-6</sup> and is well known as the TTT (time-temperature-transformation) diagram. For metallic liquids,  $\tau_1^*$  determines the critical cooling rate for glass transition. Thus, for a metallic glass-forming system, the longer the  $\tau_1^*$ , the slower the critical cooling rate to obtain a glass, and the easier the glass formation.

The internal relaxation time  $\tau_2$  is related to the intrinsic atomic activities such as structural rearrangement in any liquid.<sup>1,2,7,8</sup> It is shown both experimentally and theoretically that such a relaxation time, when properly defined, can cover a time scale of more than ten orders of magnitude, e.g., from  $10^{-13}$  (for a normal equilibrium liquid above  $T_m$ ) to  $10^2$  sec (for a deep supercooled liquid near  $T_g$ ). Thus if a liquid can be prevented from crystallization down to a temperature at which the characteristic structure relaxation time of the liquid becomes comparable to the isothermal time of the quenching process, the liquid structure would be arrested. That is, the liquid transforms into a glass.<sup>9</sup>

There exists a direct interrelationship between  $\tau_1$  and  $\tau_2$ . According to the classical homogeneous nucleation theory, only at sufficient undercooling ( $\Delta T_N$ ) could the nucleation of crystalline embryos favoring the subsequent crystal

growth become possible.<sup>1,3-6</sup> Before reaching this unique undercooling, the solidlike clusters are at nonequilibrium thermodynamically, thus no critical nucleus can form. Once  $\Delta T_N$  is approached, not only is the formation of the critical nucleus possible, but also the nucleation rate becomes explosive, followed by a steady growth of a crystalline phase. Therefore the way in which a critical nucleus is generated through thermal activations or fluctuations is closely related to the microscopic dynamics in metastable supercooled liquids.

There are plenty of recent works existing either on the atomic dynamical behaviors in supercooled liquids or on the nucleation kinetics for solidifications, most in dealing with computer simulations of simple model systems<sup>8,10-16</sup> (normally consisting of two components with different particle sizes and interaction strengths) or direct observations in colloidal and polymer systems.<sup>17-20</sup> So far there is still a lack of detailed information available on coupling the two characteristic times ( $\tau_1$  and  $\tau_2$ ) to construct a more complete picture for glass transition.<sup>8,21</sup> For computer simulations, e.g., using molecular-dynamics methods, the model system is always chosen to favor the clarification of dynamical relaxations under deep supercooling, while the crystallization is highly suppressed. As a result the corresponding  $\tau_1$  ( $\tau_1 \gg \tau_2$ ) at low temperatures may appear too long and thus far from observation within the limit of computer time.

Alternatively, it is possible to perform a detailed examination on a typical monatomic metallic model in which  $\tau_1$  and  $\tau_2$  may coincide with each other during supercooling. Thus it is much easier to bring about both nucleation and vitrification by computers using classical molecular dynamics (MD). Our purpose is to provide an atomistic understanding of how the dynamics in supercooled liquids evolves in the bifurcation of crystallization and vitrification.

**II. COMPUTATIONAL DETAILS**

Molecular dynamics in the usual classical form was performed with a monatomic system containing 3888 Cu atoms in a cubic box under three-dimensional (3D) periodic boundary conditions. The interactions among all atoms were calculated using the embedded atom method (EAM).<sup>22</sup> The poten-

tial energy of the whole system takes the form

$$E_{\text{tot}} = \sum_i F_i(\rho_i) + \frac{1}{2} \sum_{\substack{i,j \\ i \neq j}} \phi_{ij}(r_{ij}), \quad (1)$$

where  $\phi_{ij}(r_{ij})$  is a two-body central potential between atoms  $i$  and  $j$  with the separation distance  $r_{ij}$ , and  $F_i(\rho_i)$  is the embedding energy of atom  $i$  with the electron density  $\rho_i$  due to all its neighbors. We adopted the functions proposed by Mei, Davenport, and Fernando<sup>23</sup> in our calculations, except the related parameters were fitted using zero-temperature properties (the lattice constant, bulk modulus, and cohesive energy, etc.) instead of those at room temperature.<sup>24</sup> With the modified parameters of the EAM model, the equilibrium melting temperature for Cu was predicted by simulating the equilibrium condition at which the solid and liquid phases can coexist,<sup>24,30</sup>  $1320 \pm 25$  K, in reasonable agreement with the experimental value of 1352 K.

The equations of particle motion were integrated with the fifth-order predictor-corrector algorithm at a time step of  $5 \times 10^{-15}$  s. The kinetic temperature was adjusted by rescaling the particle velocities in a standard constraint manner and the total momentum of the whole system was guaranteed to be zero.<sup>25,26</sup>

The system was first equilibrated at 1800 K under a constant temperature and constant pressure (CPT) condition and subsequently cooled down to any desired temperature with a cooling rate of  $2 \times 10^{12}$  K s<sup>-1</sup>, during which the pressure was fixed to be zero. At selected temperatures, the time dependencies of both the static and the dynamical properties were studied at a constant temperature and constant volume (CVT) condition.

Specifically, the following functions<sup>27</sup> were analyzed in detail.

(i) The pair distribution function (PDF):

$$g(r) = \frac{V}{N^2} \left\langle \sum_i \sum_{j \neq i} \delta(\mathbf{r} - \mathbf{r}_{ij}) \right\rangle, \quad (2)$$

where  $\langle \dots \rangle$  means the ensemble average,  $V$  the system volume, and  $N$  the number of particles. This function gives the probability of finding a pair of atoms at a distance  $r$  apart, relative to the probability expected for a completely random distribution [with  $g(r) = 1$ ] at the same density.

(ii) The mean-square displacement (MSD):

$$\langle r^2(t) \rangle = \frac{1}{N} \sum_{i=1}^N \langle |\mathbf{r}_i(t) - \mathbf{r}_i(0)|^2 \rangle, \quad (3)$$

where  $\mathbf{r}_i(t)$  is the atomic position at time  $t$ .<sup>25</sup>

(iii) The incoherent intermediate scattering function:

$$F_s(q, t) = \frac{1}{N} \sum_{i=1}^N \langle \exp(iq \cdot [\mathbf{r}_i(t) - \mathbf{r}_i(0)]) \rangle. \quad (4)$$

This is the Fourier transform of the self-part of the Van Hove function. The wave vector  $q$  is normally selected to be the location of the first maximum in the static structure factor [Fourier transform of  $g(r)$ ], but it is shown that for other

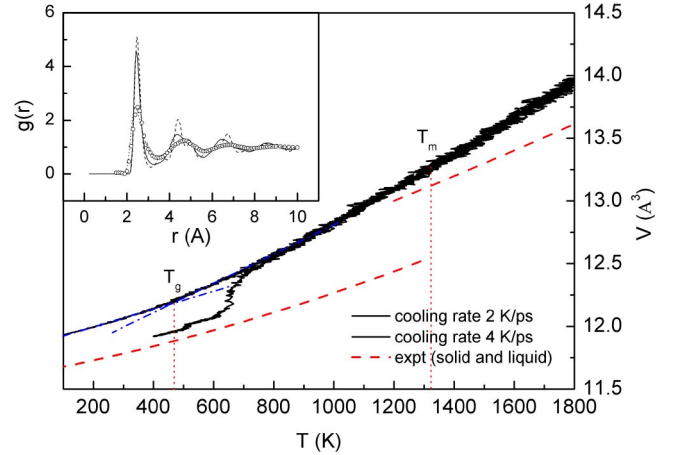


FIG. 1. Average atomic volume of Cu during cooling at different rates. This shows that the solidification temperature  $T_c$  is 650 K at a cooling rate  $\nu = 2 \times 10^{12}$  K s<sup>-1</sup> and the glass transition temperature  $T_g$  is 470 K at  $\nu = 4 \times 10^{12}$  K s<sup>-1</sup>.  $T_m = 1320$  K corresponds to the melting point of the EAM Cu. Inset: the solid line is the PDF of Cu at 300 K after glass transition; the dashed line is the PDF of Cu at 400 K after crystallization. The experimental data (open circles) and MD-calculated PDF of Cu at 1800 K (dotted line) are also given.

values of  $q$  qualitatively, a similar time and temperature dependence of  $F_s(q, t)$  is found.<sup>15</sup> This function has been used for a reasonable definition of the characteristic relaxation time for supercooled liquids and glasses.<sup>8,10-15</sup>

(iv) The non-Gaussian parameter (NGP):

$$\alpha_2(t) = 3\langle r^4(t) \rangle / 5\langle r^2(t) \rangle^2 - 1. \quad (5)$$

where  $\langle r^2(t) \rangle$  is the MSD and  $\langle r^4(t) \rangle$  is the mean quartic displacement. The NGP is related to the  $q$  dependence of the Debye-Waller factor and has been frequently used to quantify the dynamical heterogeneities of supercooled liquids and glasses.<sup>10-15,17</sup>

### III. RESULTS AND ANALYSES

Many metallic liquids are not glass formers from an experimental point of view because the critical cooling rate for glass formation is always too high to be easily accessible in experiments. However, by computer simulation, it is possible to form monometallic glasses under an extremely high cooling rate, though the glasses thus obtained are far less stable than those consisting of more than one component, e.g., the binary Lennard-Jones L-J glass formers.<sup>10-15</sup>

Two rapid quenching processes performed on the EAM Cu liquid, as measured by the  $T$  dependence of the atomic volume ( $V$ ) under a zero pressure condition, are shown in Fig. 1. In the first case, a cooling rate of  $2 \times 10^{12}$  K s<sup>-1</sup> was used. Within the temperature range 600–700 K, there is a sudden drop in  $V$  as a result of crystallization. In the second case, a merely doubled cooling rate, i.e.,  $4 \times 10^{12}$  K s<sup>-1</sup>, was used. Instead of crystallization, a glass transition has taken place during which the volume of the supercooled liquid decreases smoothly with decreasing temperature. Furthermore, the crystallization and glass transition can also be

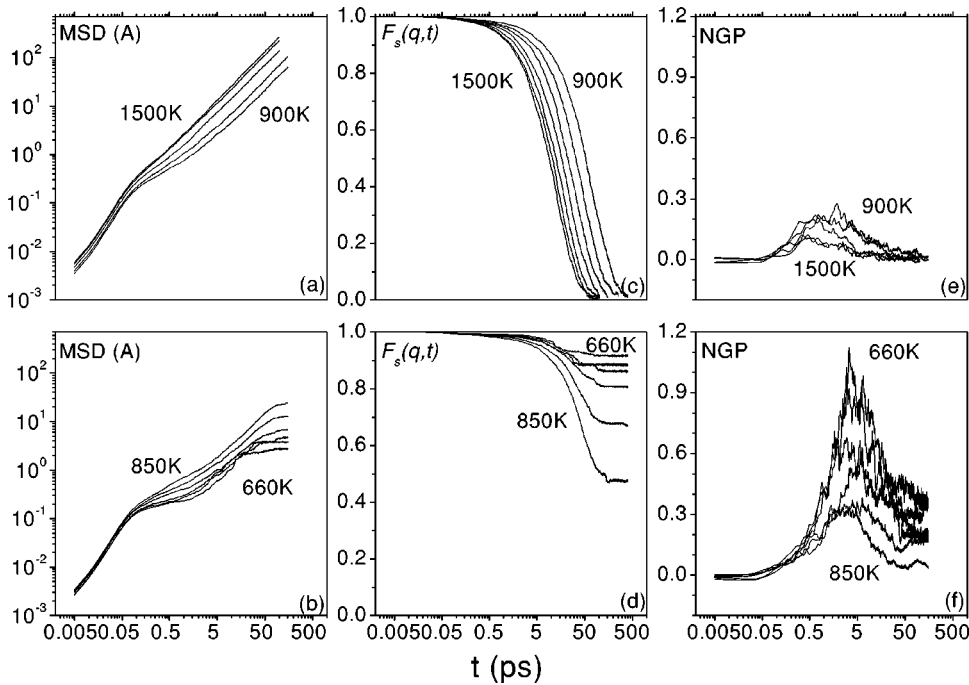


FIG. 2. Time-correlation functions at different temperatures for supercooled liquid Cu. (a) and (b) time dependencies of the MSD; (c) and (d) time dependencies of  $F_s(\mathbf{q}, t)$ ; (e) and (f) time dependencies of  $\alpha_2$ . (The higher temperatures range from 900 to 1500 K at intervals of 100 K; the lower temperatures are 850, 800, 760, 700, 680, and 660 K.)

identified by the features in the PDF's of the corresponding low-temperature products, i.e., with and without peaks characterizing the fcc crystal structure (see inset in Fig. 1). In the case of glass transition, fitting both the low- $T$  and the high- $T$  data of  $V$  linearly but separately yields a crossover at which the glass transition temperature can be determined to be 470 K, roughly one-third the melting point of Cu.

The above results demonstrate that the phase transition occurring in a supercooled liquid is very sensitive to the cooling rate or the history of supercooling. However, the  $T$  dependencies of  $V$  in each case shown in Fig. 1 do not deviate too much from one another for a large extent of the supercooling. It is within this temperature region that we performed the subsequent simulations to clarify how the microscopic dynamics evolve in supercooled liquid Cu at different temperatures. To start the simulations, we used the transient states recorded during the slower cooling process in Fig. 1 as the initial states (with  $t$  being set as zero). Instead of CPT, the system was investigated under constant volume and constant temperature (CVT) conditions. That means the volume changes related to crystallization have been neglected during our simulations. This is somewhat less realistic but will help to clarify the dynamical effects prominently.<sup>28</sup>

### A. Time-correlation functions

The time dependence of the MSD for supercooled liquid Cu for the higher ( $T \geq 900$  K) and lower ( $650 < T < 900$  K) temperatures is plotted in Figs. 2(a) and 2(b), respectively. At high temperatures, the MSD curves are typical for simple liquids.<sup>15</sup> For short times, the MSD increases with time as  $\langle r^2 \rangle \propto t^2$  due to ballistic motion of atoms. For longer times, the atomic motion becomes diffusive and  $\langle r^2 \rangle \propto t$ . At intermediate times, a plateau appears, which is more pronounced at lower temperatures. The occurrence of the plateau results from the so-called “cage effect” for a tagged particle, i.e., it

takes some time for a particle to escape from the “cage” formed by its surrounding neighbors. The lower the temperature, the longer the time required, thus the more distinct the plateau. In mode-coupling theory (MCT),<sup>12–14</sup> the time window close to the plateau is usually called the “ $\beta$ -relaxation regime” and the window in which the correlation functions fall below the plateau the “ $\alpha$ -relaxation regime”.

For low- $T$  cases [Fig. 2(b)], the situation is quite different within the same statistic time region from that for high  $T$  [Fig. 2(a)]. Each of these MSD curves shows a second plateau that emerges after entering the  $\alpha$ -relaxation regime. Both the onset time and the height of the second plateaus decrease with decreasing  $T$ . Further investigation revealed that the presence of the second plateau is the result of the nucleation and growth of the crystalline phase, which will be discussed in the following sections with details. According to the Einstein relation, i.e.,  $\langle r^2(t) \rangle = 6Dt$ , the self-diffusion coefficient  $D$  can be calculated from the slope of the linear fitting of the MSD, given the time is long enough. Obviously, when the MSD behaves as a plateau,  $D$  tends to be zero, a result of the structural arrest. Within the time windows we examined here, the occurrence of a dynamical transformation from that of a normal (supercooled) liquid to the one prior to nucleation can be identified.

Further evidence supporting the above conclusion are the  $T$  dependencies of other time-correlation functions, i.e.,  $F_s(\mathbf{q}, t)$  and the NGP, shown along with the MSD curves in Fig. 2. During the calculation of  $F_s(\mathbf{q}, t)$ , the value of the wave vector  $q$  was set as the position of the first peak in the PDF of equilibrium liquid Cu at  $T = 1800$  K (the inset of Fig. 1). The plots shown in Figs. 2(c) and 2(d) demonstrate that, in accordance with those MSD observations, each  $F_s(\mathbf{q}, t)$  curve at high  $T$  can decay to a nearly zero value given sufficient relaxation time, implying that metastable liquids still follow the relaxation dynamics of normal liquids. While at

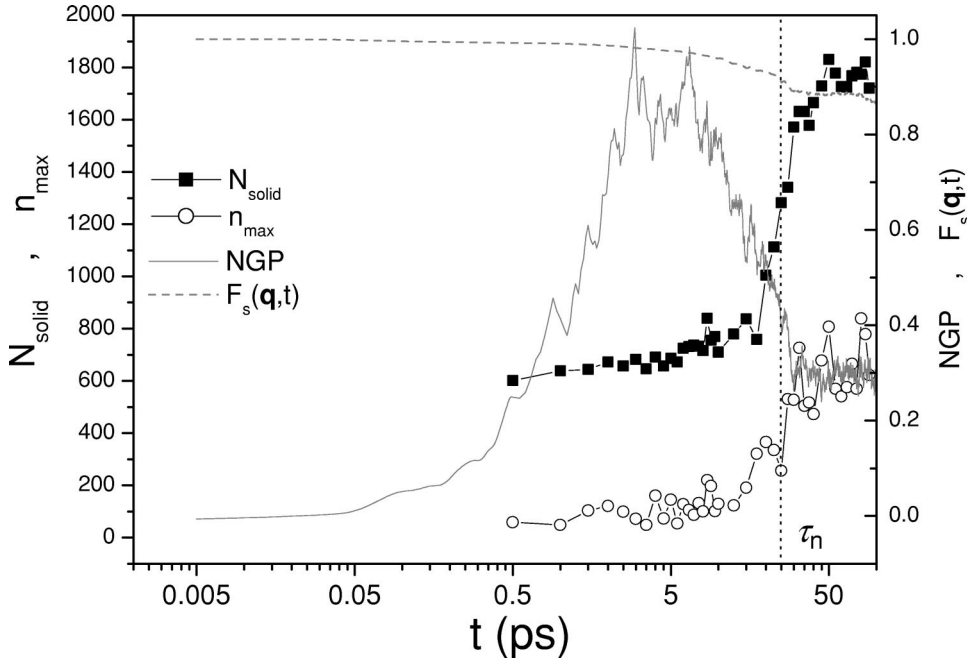


FIG. 3. The total of solidlike Cu atoms  $N_{\text{solid}}$  and the number of atoms in the maximum solid cluster  $n_{\text{max}}$  vs time when relaxation is at  $T=700$  K. Also plotted is the NGP and  $F_s(\mathbf{q},t)$  vs  $t$  at the same temperature.

low temperatures, the liquid is less (meta-) stable and the massive structural rearrangements will soon lead to nucleation and stagnate the dynamics of the liquid. So instead of decaying to zero, the  $F_s(q,t)$  shows a plateau with further increasing time. Note that the onset time of such a plateau is exactly equal to that of the second plateau in the MSD curve at the same  $T$ .

The same occurs to the  $T$  dependence of the NGP [Figs. 2(e) and 2(f)]. Starting from  $\alpha_2(t=0)=0$ , all the NGP curves rise in the time scale of the  $\beta$ -relaxation regime. Then for high  $T$ , the NGP drops on the time scale of  $\alpha$  relaxation, and finally drops to nearly zero, the result of the ergodicity of the system at a sufficiently long time [corresponding to the limit of  $F_s(q,t \rightarrow \infty)=0$ ]. An increase of the peak with decreasing  $T$  implies a more pronounced heterogeneity of the relaxations as the system is cooled.<sup>10–15,17,29,30</sup> While at low  $T$ , the NGP curve will also show a maximum, but it can be interrupted by a nonzero plateau during its dropping, and the lower the temperature the higher the plateau.

Variations of all the time-correlation functions are quite consistent with each other at different temperatures. Two dynamical behaviors of supercooled liquid Cu can be clarified. When  $T$  is higher than 900 K, the system can undergo  $\beta$ - and  $\alpha$ -relaxation regimes like normal simple liquids, and the atoms exhibit diffusive rearrangements. When  $T$  is lower than 900 K, besides the normal  $\beta$  and  $\alpha$  relaxation, a third stage occurs shortly after entering the  $\alpha$ -relaxation regime. As a result, the nondiffusive rearrangements occur at a typical time scale of about 50 ps (neglecting the cooling time, see Sec. III C for details), almost one order-of-magnitude longer than the onset time of the  $\alpha$ -relaxation region ( $\sim 5$  ps).

### B. Static snapshot analysis

The heterogeneity of the relaxations implies that the dynamics of the system is collective on an atomic scale, i.e., when a tagged atom tends to move faster (or slow down), so

do its neighbors. The question is how the collective motion evolves during the different stages of those structural relaxations.

For this purpose, we recorded snapshots at different relaxation times and temperatures and analyzed them. In the following we only provide results taken at  $T=700$  K as an example. For other configurations at different  $T$  the pictures are similar.

Two methods were chosen to characterize the atomic relaxation activities. In the first method, we distinguish the crystallized atoms from the liquid ones. In previous simulation studies, different criteria have been used to identify solidlike atoms, among which the one proposed by ten Wolde *et al.*<sup>32,33</sup> is independent of the *a priori* assumption about the structure of the solidlike cluster; this criterion was adopted in this paper. To be brief, the local structure around particle  $i$  can be characterized by a set of order parameters  $\bar{q}_{lm}(i) \equiv [1/N_b(i)] \sum_{j=1}^{N_b(i)} Y_{lm}(\hat{r}_{ij})$ , where  $Y_{lm}(\hat{r}_{ij})$  are spherical harmonics,  $\hat{r}_{ij}$  is a unit vector in the direction of the bond between particle  $i$  and its neighbor  $j$ , and the sum runs over all its  $N_b$  neighbors. Based on  $\bar{q}_{lm}(i)$ , a dot product of the normalized vectors  $\mathbf{q}_l$  of neighboring particles  $i$  and  $j$  is defined as  $\mathbf{q}_l(i) \cdot \mathbf{q}_l(j) \equiv \sum_{m=-l}^l \bar{q}_{lm}(i) \bar{q}_{lm}(j)^*$ , where the component  $\bar{q}_{lm}(i)$  is proportional to  $\bar{q}_{lm}(i)$ . Clearly,  $\mathbf{q}_6(i) \cdot \mathbf{q}_6(i) = 1$ . We consider two particles to be “connected” if  $\mathbf{q}_6(i) \cdot \mathbf{q}_6(j) > 0.5$ . Under such a strategy, a particle will be identified as “solidlike” if the number of connections with its neighboring particles exceeds 11 (there are 12 neighbors for each atom in the fcc lattice). Furthermore, if the distance between a pair of atoms is less than the first-neighbor distance (corresponding to the location of the first minimum of the PDF averaged for the same snapshot), we define the two particles as belonging to the same cluster.

Then we made a survey of how the number of those solidlike atoms as defined above evolves during the relaxations. In Fig. 3 we illustrate the time dependence of all the solidlike

atoms ( $N_{\text{solid}}$ ) in the system and the number of atoms in the maximum solid cluster ( $n_{\text{max}}$ ) at that time. We also plotted the time-correlation functions for comparison purposes. During the time scale of  $\beta$ -relaxation regime, though  $N_{\text{solid}}$  increases with time, it remains small in the supercooled liquid (less than 20%).  $n_{\text{max}}$  fluctuates during this time region. On entering  $\alpha$  relaxation, both  $N_{\text{solid}}$  and  $n_{\text{max}}$  increase steadily for a short time and increase abruptly at a certain critical time. After the saltation, the increasing of  $n_{\text{max}}$  and  $N_{\text{solid}}$  slows down again, during which all the time-correlation functions manifest themselves as a shoulder (or nonzero plateau), a result of postnucleation growth of the crystalline phase.

It is worth noting that the time corresponding to the abrupt increase of  $n_{\text{max}}$  is in good agreement with the onset time of the dynamics transition in crystallization (denoted as  $\tau_n$  in Fig. 3). By classical nucleation theory, only those clusters, which are larger than the critical nuclei, can grow steadily. Therefore, it is reasonable to determine the sudden rise of  $n_{\text{max}}$  as a result of the growing up of the critical nucleus. In other words, the critical size should be no larger than  $n_{\text{max}}$  at the critical time. For our simulations, the critical size thus defined is about 200 atoms at  $650 < T < 900$  K, nearly 5% of the whole system. It also confirms that the finite-size effects of the simulation box can be negligible.

In the second method, we divided these solidlike atoms into two different kinds of groups according to the atomic displacement  $\Delta r_i(t) = |r_i(t) - r_i(0)|$ . At any transient time  $t$ , the average of the mean displacement of all the atoms in the system was calculated by  $\Delta r(t) = 1/N \sum_i \Delta r_i(t)$ . If  $\Delta r_i(t) > \Delta r(t)$ , atom  $i$  is regarded as “fast moving” or “mobile,” otherwise, it is “slow moving” or “immobile.” Then we determined those clusters constructed with only mobile atoms and only immobile atoms. By doing this, the collective manner of either mobile or immobile atoms can be clarified.

The main observations are as follows. (i) At the early stage of the structural relaxations, the mobile atoms appear more collectively than do the immobile ones. The clusters consisting of mobile atoms emerge randomly with a small size of about ten atoms. This was shown in Fig. 4(a) with 3D plotting. (ii) With further increasing time, there is no indication for further growth of those clusters formed by mobile atoms; instead, the correlation among immobile atoms becomes much stronger. Meanwhile, atoms within these appear to be ordered [cf. Fig. 4(b)]. (iii) At even longer times, those clusters associated with the immobile atoms become even larger and more stable. They merge and spread throughout the MD box, an indication of nucleation and growth of the crystalline phase. Within this stage and afterwards, the correlation among mobile atoms also becomes stronger the more atoms are involved [Figs. 4(c) and 4(d)].

The onset of nucleation seems to be a direct consequence of the heterogeneous dynamics: once the atoms find their more stable local configurations via moving fast, they slow down. First the ordered portions are randomly distributed within the system and then they coalesce with a significant collective appearance of fast-moving atoms at their boundaries. This may be due to the fact that different crystal nuclei may show different crystalline orientations; it is favorable to

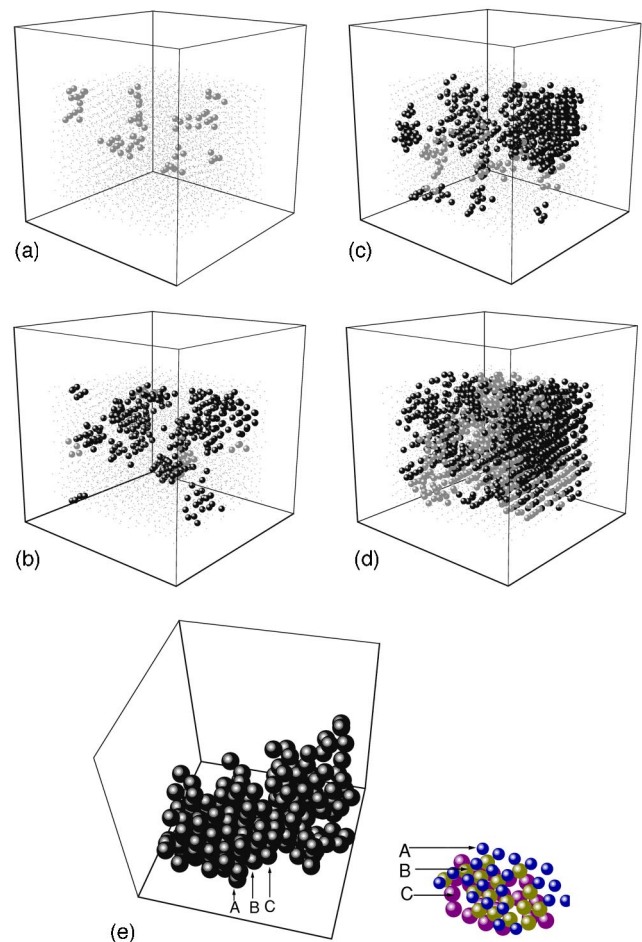


FIG. 4. Snapshots of clusters formed by mobile (gray) and immobile (dark) solidlike Cu atoms at different relaxation times for  $T=700$  K. The rest atoms are little light gray spheres. (a)  $t = 0.03\tau_n$ ; (b)  $t = 0.4\tau_n$ ; (c)  $t = 1.0\tau_n$ ; (d)  $t = 2.0\tau_n$ ; (e) the largest cluster formed by solidlike atoms after relaxation for  $0.4\tau_n$ . This cluster contains 214 atoms. The remaining atoms are not shown. Inset: The segments of layers A–C in the cluster, showing that the stacking in this figure is fcc-like (that is, ABC stacking).

readjust their orientations when they meet with each other, in order to minimize the total free energy at their boundaries.

The results provide little evidence of preexisting crystal nuclei in the present MD cooling process. Facilitated by the collective fluctuations of those fast-moving atoms, the nuclei tend to form after sufficient relaxation time. This behavior is distinct from that of a Ni supercooled liquid,<sup>31</sup> in which during rapid quenching clusters with preexisting crystalline orders can be detected and they grow simultaneously with the decreasing  $T$  (also known as quenched-in nuclei).

Our method as explained above is able to distinguish the role of fast-/slow-moving atoms in the dynamics transition from relaxation to crystallization. Since  $\Delta r_i(t)$  is recorded from the same initial time as when the time-correlation functions are calculated, it provides a fully consistent picture of the temporal dynamical consequence in the same manner as any of those of the time-correlation functions.

In our simulation, no indication of bcc-like ordering appears prior to the fcc one during the initial stage of nucle-

ation. The fcc local ordering immediately follows the local collective activity. Previous observations of the nucleation of the fcc phase being facilitated by the less stable bcc-type ordering, either within those incipient nuclei<sup>31,32</sup> or at their boundaries,<sup>33</sup> may be a result of different properties of potentials. It is also noted that the shape of any nucleus, whether it is subcritically sized or critically sized, is highly irregular. Furthermore, the crystal clusters show (111) stacking of the fcc structure [Fig. 4(e)]. This is in accordance with many other studies concerning the way in which a solid phase is nucleated from a supercooled liquid phase.<sup>18</sup>

Through these static snapshot analyses, we conclude that it is only after a certain time ( $\tau_n$ ) can the nuclei for crystal growth be formed, i.e., there exists a distinct dynamically originated transition that combines the structural relaxations of the metastable supercooled liquid with nucleation and growth kinetics of any crystalline phase. Such a transformation can be quantitatively identified and it is directly related to the dynamical heterogeneity in a supercooled liquid.

### C. Relaxation, nucleation, and glass transition

In this section, we discuss the relationship among relaxation, nucleation, and glass transition by considering the related characteristic time scales. For any supercooled liquids, we quantify the following two characteristic relaxation times.

(i) The characteristic structural relaxation time  $\tau_\alpha$  or the  $\alpha$ -relaxation time, which is defined as the time when the correlation function  $F_s(q, t)$  has decayed to  $e^{-1}$ .<sup>10-15</sup>

(ii) The characteristic time of nucleation and crystallization  $\tau_n$ , which corresponds to the breakdown of the typical structural relaxation dynamics in metastable liquids, and signals the onset of the formation of the critical nucleus and subsequent growth of crystals.

At high  $T$ , i.e.,  $900 < T < 1500$  K, no crystallization can be detected in our system (e.g., within a MD time as long as 1 ns at  $T=1000$  K), indicating the stability of the supercooled liquid (metastable). The  $\tau_\alpha$  increases with decreasing  $T$ . According to the idealized MCT, the temperature dependence of  $\tau_\alpha$  follows a power law  $\tau_\alpha \propto (T - T_c)^{-\lambda}$  for supercooled simple liquids, where  $T_c$  is the temperature at which the system undergoes a transition from ergodic to nonergodic behavior.<sup>34</sup> Usually for a model glass-forming system, e.g., binary L-J liquids, the exponent parameter  $\lambda$  is estimated<sup>12-14</sup> to be  $2 < \lambda < 3$ . Fitting our  $\tau_\alpha$  data as a function of  $T$  under this power-law scheme yields  $\lambda \approx 3.07, 2.37$ , and 1.65 for  $T_c = 200, 400$ , and 600 K, respectively. The results are illustrated in Fig. 5. If we take the ideal mode-coupling critical point to be 600 K, the much lower exponent (1.65) than the L-J ones indicates that the supercooled liquid copper is more fragile than the L-J binary liquids, or its glass-forming ability is much less strong. Otherwise, if we assume the Cu liquid follows exactly the same exponent as the L-J one (e.g., taking  $\lambda \approx 3.07$  as a universal scaling parameter), the corresponding  $T_c$  is 200 K indicates a very low mode-coupling critical point, with an even lower ideal glass transition temperature—also suggesting a rather weak glass-

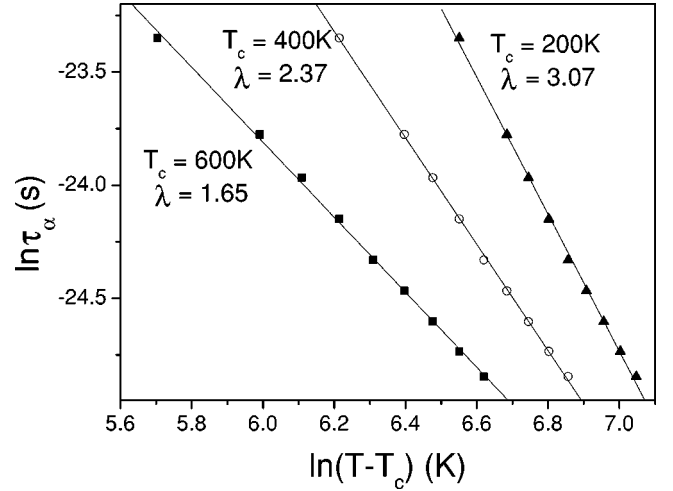


FIG. 5. Temperature dependence of  $\tau_\alpha$ , fitted by  $(T - T_c)^{-\lambda}$  and plotted log-log to reveal a power-law dependence. When  $T_c = 200$  K (filled triangles), 400 K (open circles), and 600 K (filled squares), the fitted  $\lambda = 3.07, 2.37$ , and 1.65, respectively.

forming ability. This is quite consistent with our observation that the cooling rate needs to be extremely high to bring the Cu liquid into a glassy state.

On the other hand,  $\tau_n$  appears to be detectable only at temperatures below 900 K in our simulations, and it decreases with decreasing temperature. The history of supercooling is not included in  $\tau_n$ . To include it, one must add a time correction  $\Delta\tau$ , which corresponds to the amount of time the system has been away from the equilibrium state at the melting point 1350 K, and it can be estimated according to the extent of supercooling and the cooling rate. The characteristic time of  $\tau_n$  after the correction is denoted as  $\tau'_n$ , i.e.,  $\tau'_n = \tau_n + \Delta\tau$ .

Both  $\tau'_n$  and  $\tau_n$  are shown in Fig. 6 (and the inset), together with  $\tau_\alpha$ , to illustrate their  $T$  dependence. Clearly, upon increasing supercooling,  $\tau'_n$  decreases and reaches a minimum, following a nonmonotonic relationship with  $T$  in a way closely resembling the typical TTT diagram. Thus it is clear that the time  $\tau'_n$  is similar to  $\tau_1$  as explained in the introduction, and  $\tau_\alpha$  is equivalent to  $\tau_2$ .

Our result also provides a link between  $\tau_\alpha$  (or  $\tau_2$ ) and  $\tau'_n$  (or  $\tau_1$ ). As we have already pointed out, the crystallization (nucleation and growth) is facilitated in the  $\alpha$ -relaxation region. Extrapolating the MD data of  $\tau_\alpha$  according to the power-law fittings shown in Fig. 5, we get a crossover with  $\tau'_n$ , underlying the existence of an upper time limit for  $\tau_\alpha$  below which the liquid could be supercooled down to the crossover temperature while preventing the nucleation and growth of the crystalline phase. Though the uncertainty in  $T_c$  appears to be large ( $400 \pm 200$  K, as shown in Fig. 1), the times are quite close to each other at those crossovers and quite close to the minimum nucleation time. For convenience, we take the intermediate case ( $T_c = 400$  K) as an example. The time and temperature at the crossover read approximately 360 ps (denoted as  $\tau_1^*$  in the introduction) and 635 K, respectively. This yields a critical cooling rate of 2.0 K ps<sup>-1</sup>—the ratio of the supercooling (1350–635 K) over

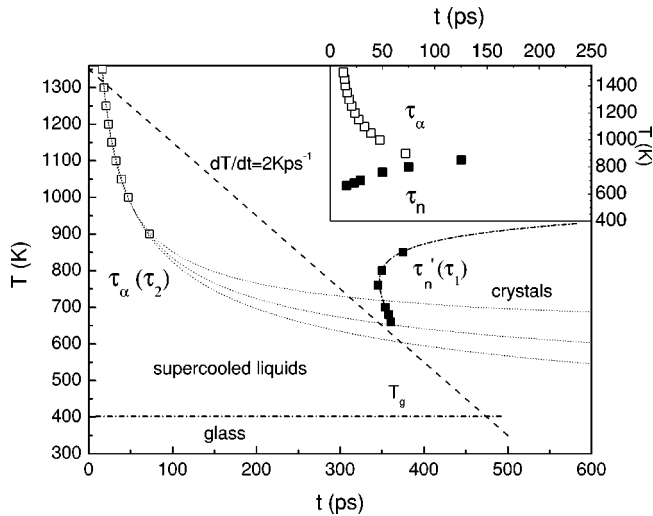


FIG. 6. Temperature dependence of  $\tau_\alpha$  (open squares) and  $\tau'_n$  (filled squares).  $\tau_\alpha$  and  $\tau'_n$  have been rescaled. The dotted curves are the extrapolations of  $T$ - $\tau_\alpha$  fitted by  $\tau_\alpha \propto (T - T_c)^{-\lambda}$  with  $T_c = 200, 400,$  and  $600$  K from top to bottom. The dash-dotted curve is the fitted  $T$ - $\tau'_n$ . The dashed line  $dT/dt$  denotes the cooling rate of  $2 \text{ K ps}^{-1}$ . The time and temperature of the crossover of  $T$ - $\tau'_n$  and  $T$ - $\tau_\alpha$  for  $T_c = 400$  K approximate to be  $635$  K and  $360$  ps, which denotes a critical cooling rate of  $2 \text{ K ps}^{-1}$  for glass transition. Inset: Temperature dependence of  $\tau_\alpha$  and  $\tau_n$  without time correction.

time  $\tau_1^*$  ( $360$  ps)—within uncertainty. This is exactly the cooling rate ( $2 \text{ K ps}^{-1}$ , also indicated in Fig. 6) at which the supercooled liquid Cu was obtained and analyzed. Recall that in Fig. 1, under such a cooling rate, the system will crystallize at about  $650$  K (the slight difference of the crystallization temperature may be due to the fact that both  $\tau_\alpha$

and  $\tau_n$  were determined under a constant volume condition); via a higher cooling rate ( $4 \text{ K ps}^{-1}$ ), the system will undergo a glass transition—consistent with our prediction.

The time  $\tau'_n$  appears to be very long above  $1000$  K. This is in accordance with the prediction of a critical undercooling ( $\Delta T_N$ ) in terms of the homogeneous nucleation theory. The literature reported that  $\Delta T_N$  for Cu (Ref. 36) is about  $240$  K, which is about half of our MD results.

#### IV. CONCLUSIONS

Structural relaxations in supercooled liquid Cu were studied with the MD and the EAM potentials. Characteristic relaxation times were determined based on examinations of several time-correlation functions. Within the typical  $\alpha$ -relaxation regime the structural rearrangement acts as a leading factor to induce the incipient nucleation, underlying the existence of a transition in dynamical heterogeneities.

From the  $T$  dependence of both the  $\alpha$ -relaxation time ( $\tau_\alpha$ ) and the characteristic time for nucleated crystallization ( $\tau'_n$ ), a time-temperature-nucleation diagram can be constructed. All results appear to be consistent under such a picture, in the way that relaxation, nucleation, and glass transition are shown to be closely correlated with each other. Our results confirm again that the  $T$  dependence of the  $\alpha$ -relaxation time ( $\tau_\alpha$ ) itself serves as a direct and reliable measure of the glass-forming ability, for both model and real systems.<sup>7,35,36</sup>

#### ACKNOWLEDGMENTS

The authors thank Dr. E. Ma for many useful discussions. This work was supported by the NSFC (Grant Nos. 59841004 and 50021101) and the Max-Planck Society of Germany.

\*Electronic address: hpan@mf.mpg.de

<sup>1</sup>P. G. Debenedetti, *Metastable Liquids—Concepts and Principles* (Princeton University, Princeton, NJ, 1996).

<sup>2</sup>C. A. Angell, *Science* **267**, 1924 (1995).

<sup>3</sup>D. Turnbull, *Contemp. Phys.* **10**, 473 (1969).

<sup>4</sup>A. L. Greer, *Science* **267**, 1947 (1995).

<sup>5</sup>D. R. Uhlmann, *J. Non-Cryst. Solids* **7**, 337 (1972).

<sup>6</sup>W. B. Hillig and D. Turnbull, *J. Chem. Phys.* **24**, 914 (1956).

<sup>7</sup>See, for example, the special issue on glasses and glass-forming liquids [*Science* **267** (1995)]; M. D. Ediger, C. A. Angell, and S. R. Nagel, *J. Phys. Chem.* **100**, 13 200 (1996).

<sup>8</sup>P. G. Debenedetti and F. H. Stillinger, *Nature (London)* **410**, 259 (2001).

<sup>9</sup>J. H. Gibbs and E. A. DiMarzio, *J. Chem. Phys.* **28**, 373 (1958).

<sup>10</sup>W. Kob and H. C. Andersen, *Phys. Rev. Lett.* **73**, 1376 (1994); *Phys. Rev. E* **51**, 4626 (1995); **52**, 4134 (1995).

<sup>11</sup>W. Kob, C. Donati, S. J. Plimpton, P. H. Poole, and S. C. Glotzer, *Phys. Rev. Lett.* **79**, 2827 (1997).

<sup>12</sup>C. Donati, S. C. Glotzer, P. H. Poole, W. Kob, and S. J. Plimpton, *Phys. Rev. E* **60**, 3107 (1999).

<sup>13</sup>S. C. Glotzer and C. Donati, *J. Phys.: Condens. Matter* **11**, A285 (1999).

<sup>14</sup>P. H. Poole, S. C. Glotzer, A. Coniglio, and N. Jan, *Phys. Rev. Lett.* **78**, 3394 (1997).

<sup>15</sup>W. Kob, *J. Phys.: Condens. Matter* **11**, R85 (1999).

<sup>16</sup>S. Sastry, *Nature (London)* **409**, 164 (2001).

<sup>17</sup>E. R. Weeks, J. C. Crocker, A. C. Levitt, A. Schofield, and D. A. Weitz, *Science* **287**, 627 (2000).

<sup>18</sup>U. Gasser, E. R. Weeks, A. Schofield, P. N. Pusey, and D. A. Weitz, *Science* **292**, 258 (2001).

<sup>19</sup>L. A. Deschenes and D. A. Vanden, *Science* **292**, 255 (2001).

<sup>20</sup>M. E. Cates and M. R. Evans, *Soft and Fragile Matter* (Institute of Physics, University of Reading, Berkshire, 2000).

<sup>21</sup>C. A. Angell, *J. Phys.: Condens. Matter* **12**, 6463 (2000).

<sup>22</sup>M. S. Daw and M. I. Baskes, *Phys. Rev. Lett.* **50**, 1285 (1983); *Phys. Rev. B* **29**, 6443 (1984).

<sup>23</sup>J. Mei, J. W. Davenport, and G. W. Fernando, *Phys. Rev. B* **43**, 4653 (1991).

<sup>24</sup>F. T. Xu, Z. H. Jin, J. Zhong, and K. Lu, *Sci. China, Ser. E: Technol. Sci.* **44**, 432 (2001).

<sup>25</sup>M. P. Allen and D. J. Tildesley, *Computer Simulation of Liquids* (Oxford University, New York, 1989).

<sup>26</sup>D. Frenkel and B. Smit, *Understanding Molecular Simulations* (Academic, New York, 1996).

<sup>27</sup>J.-P. Hansen and I. R. McDonald, *Theory of Simple Liquids* (Academic, London, 1986).

<sup>28</sup>K. Vollmayr, W. Kob, and K. Binder, *Phys. Rev. B* **54**, 15 808 (1996).

<sup>29</sup>R. Yanamoto and A. Onuki, *Phys. Rev. Lett.* **81**, 4915 (1998).

- <sup>30</sup>Z. H. Jin, P. Gumbsch, K. Lu, and E. Ma, Phys. Rev. Lett. **87**, 055703 (2001).
- <sup>31</sup>S. Alexander and J. P. McTague, Phys. Rev. Lett. **41**, 702 (1978).
- <sup>32</sup>P. R. ten Wolde, M. J. Ruiz-Montero, and D. Frenkel, J. Chem. Phys. **104**, 9932 (1996).
- <sup>33</sup>P. R. ten Wolde, M. J. Ruiz-Montero, and D. Frenkel, Phys. Rev. Lett. **75**, 2714 (1995).
- <sup>34</sup>W. Götze and L. Sjögren, Rep. Prog. Phys. **55**, 241 (1992).
- <sup>35</sup>H. Wendt and R. Richert, Phys. Rev. E **61**, 1722 (2000).
- <sup>36</sup>C. A. Angell, K. L. Ngai, G. B. McKenna, P. F. McMillan, and S. W. Martin, J. Appl. Phys. **88**, 3113 (2000).